

Dynamics and Control of Instrumented Harmonic Drives

H. Kazerooni

Mechanical Engineering Department,
University of California,
Berkeley, CA 94720

Since torque in harmonic drives is transmitted by a pure couple, harmonic drives do not generate radial forces and therefore can be instrumented with torque sensors without interference from radial forces. The installation of torque sensors on the stationary component of harmonic drives (the Flexipline cup in this research work) produce backdrivability needed for robotic and telerobotic compliant maneuvers [3, 4, 6]. Backdrivability of a harmonic drive, when used as torque increaser, means that the output shaft can be rotated via finite amount of torque. A high ratio harmonic drive is non-backdrivable because its output shaft cannot be turned by applying a torque on it. This article first develops the dynamic behavior of a harmonic drive, in particular the non-backdrivability, in terms of a sensitivity transfer function. The instrumentation of the harmonic drive with torque sensor is then described. This leads to a description of the control architecture which allows modulation of the sensitivity transfer function within the limits established by the closed-loop stability. A set of experiments on an active hand controller, powered by a DC motor coupled to an instrumented harmonic drive, is given to exhibit this method's limitations.

1 Introduction

Developed over 30 years ago primarily for aerospace applications, harmonic drives are compact transmission systems which increase the torque of electric motors. With increase use of robotics, back-drivable harmonic drives can be employed in robotic compliant maneuvers. Harmonic drives consist of three simple parts and thus offer practitioners the freedom to incorporate drive components into machines or equipment. This article first gives a summary of the harmonic drive's principle of operation. Section 3 discusses the dynamic behavior of the harmonic drive where it is shown that large reduction ratios (usually more than 60) result in non-backdrivable systems [4]. This leads to a discussion of the sensors required to make the harmonic drive arbitrarily backdrivable. Section 4 develops the control

Harmonic drives have three elements [2]: 1) Elliptical Wave Generator, 2) Flexipline (or Cup), and 3) Rigid Circular Spline (Fig. 1). The Elliptical Wave Generator is an elliptical bearing attached to the motor drive shaft. The Flexipline is a nonrigid cup whose inner surface grasps the Wave Generator at the cup's open end. The Flexipline's edge conforms to the Wave Generator's elliptical shape as the Generator rotates. The Flexipline's outer surface has teeth which contact the internal teeth of the Rigid Circular Spline, a rigid ring. The Flexipline has two fewer teeth than the Rigid Circular Spline. Thus, one revolution of the Wave Generator will cause relative motion between the Rigid Circular Spline and the Flexipline.

Suppose n_f is the number of teeth on the Flexipline, and

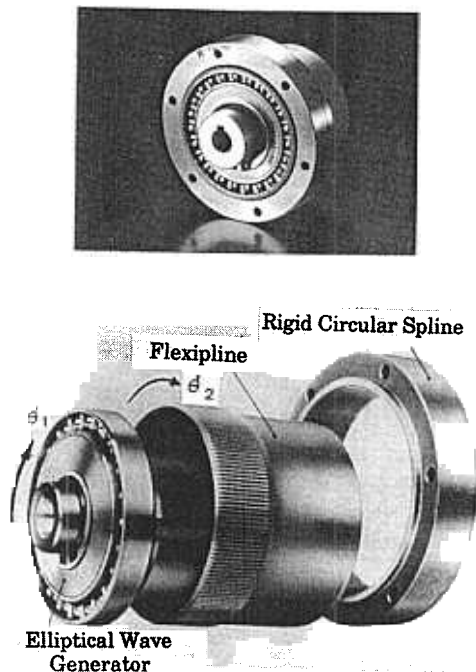


Fig. 1 Harmonic drive components. When the flexipline is kept stationary, the elliptical wave generator and the rigid circular spline rotate at the same direction.

Circular Spline is considered to be the output and rotates such that the reduction ratio, r , is determined by:

$$r = 1 - \frac{n_f}{n_f - n_r} \quad (2)$$

The ratio in this case is positive and the Rigid Circular Spline and Wave Generator rotate at the same direction. If $n_f = 400$, and $n_r = 402$, then Eq. (2) results in $r = 201$. The analysis on this paper is for the latter case where the Flexipline is stationary and Rigid Circular Spline rotates the load.¹ The holes in the Rigid Circular Spline fasten to the load.

3 Dynamic Behavior

This section describes the dynamic behavior of the harmonic drive. At this point no assumptions are made about the type of control employed for the motor that drives the Wave Generator. The Wave Generator is coupled directly to the motor shaft while the Flexipline is held stationary and the Rigid Circular Spline is employed to maneuver a load. $U(s)$, the voltage command to the motor amplifier, is the input. $\theta_1(s)$, the motor position (or the Wave Generator position), is the output. The transfer function $G(s)$ represents the motor dynamics.

$$\theta_1(s) = G(s) U(s) \quad (3)$$

No assumptions on the structure or order of G^2 are made at this point. All dynamic characteristics associated with the DC motor including the friction torque is implicitly incorporated in $G(s)$. Suppose the Rigid Circular Spline is

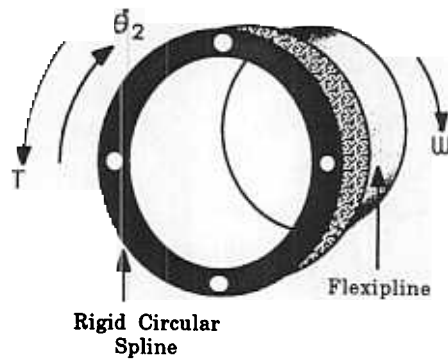


Fig. 2 The circular rigid spline and the flexipline. The flexipline is held stationary and the rigid circular spline rotates with a speed of $\dot{\theta}_2$.

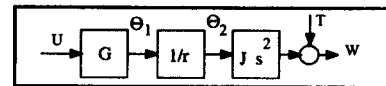


Fig. 3 The dynamic behavior of the harmonic drive maneuvering a mass with moment of inertia of J

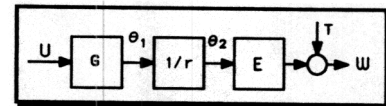


Fig. 4 The general representation of the dynamic behavior of the harmonic drive when rigid circular spline interacts with the environment E

employed to drive a load whose inertia is J . Inspection of Figure 2 results in the following equation for the dynamic behavior of the assembled Flexipline and the Rigid Circular Spline:

$$W - T = J \ddot{\theta}_2 \quad (4)$$

W is the torque that holds the Flexipline stationary. T is all possible external torques that oppose the motion of the Rigid Circular Spline (and its load).

Assuming $\dot{\theta}_1 = r\dot{\theta}_2$, the block diagram of Fig. 3 depicts one possible combination of Eqs. (3) and (4) which can represent the dynamic behavior of the harmonic drive when maneuvering a load with inertia of J . Inspection of the block-diagram of Fig. 3 shows that the torque that holds the flexipline, W , results from two independent variables: 1) the input voltage command to the amplifier input, 2) all torques that oppose the motion of the load. The block diagram of Fig. 3 also depicts the non-backdrivability of the system where T does not affect θ_2 ; it only adds to W .

If the Rigid Circular Spline and load with inertia J were in contact with an environment with stiffness and damping of K and C , the block diagram of Figure 3 should be modified as given Fig. 4 where $E(s) = Js^2 + Cs + K$. Note that E can be any arbitrary dynamics representing the dynamics of the Rigid Circular Spline and its interacting environment. In particular, we are interested in powered hand controllers for telerobotic applications where a human is in contact with a stick driven by a Rigid Circular Spline. (Section 6 will give a more detailed description about the hand controller.) K ,

¹This is the most commonly used configuration in robotics. The derivations in this article can be extended to other configurations also.

²The Laplace argument of various variables, s , are given only when the variables are introduced for the first time.

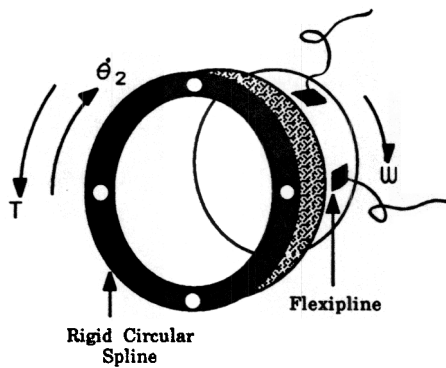


Fig. 5 Four strain gages on the flexipline support measures ω

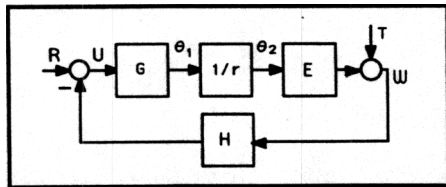


Fig. 6 The torque keeping the flexipline stationary is used as a feedback to make the system backdrivable

C , and J in the case of a hand controller represent the dynamic behavior of the human hand and the stick as seen from the Rigid Circular Spline. See reference [5] for an example in measurement of E for the human arm.

4 Instrumentation and Control

Our primary purpose is to develop an instrumentation which allows a designer to modify arbitrarily the behavior of the harmonic drive so it responds to the external torques T and becomes backdrivable. We suggest that W , the torque that holds the Flexipline stationary, be measured by installing four strain gages on either the Flexipline or the structure that holds the Flexipline [8]. Since the Flexipline is stationary, the measurement of W is rather straightforward. This torque, after modification by a controller, is then used to drive the motor in the direction of T . Measuring joint torque on a rotating shaft in robotic systems has always been difficult for engineers. This design allows measurement of joint torques from a stationary part, the Flexipline cup.

Figure 6 shows the control architecture where the measured torque W is used to drive the motor after compensation by $H(s)$, and $R(s)$ is the input command. Inspection of Fig. 6 results in the following equation for θ_2 .

$$\theta_2 = P(s)R - S(s)T \quad (5)$$

where the transfer function P and S are given as:

$$P = \frac{\frac{G}{r}}{1 + \frac{GHE}{r}} \quad (6)$$

$$S = \frac{\frac{GH}{r}}{1 + \frac{GHE}{r}} \quad (7)$$

S is defined as the system *sensitivity transfer function* ($1/\text{impedance}$). Designers can shape the sensitivity transfer function via selection of a proper H via any standard linear controller design method. For brevity, the selection of the compensator, H is not discussed here; reference [1] gives the best description of such control methods.

Here we discuss a few properties of closed loop system. Inspection of Eq. (5), (6), and (7) reveals that when H is small, T does not affect θ_2 , the output motion, because S approaches zero. The system is therefore non-backdrivable. When H becomes very large (i.e., approaches infinity) over a finite frequency range, then P approaches zero and θ_2 from Eq. (5) will be a function of T only:

$$\theta_2 = -\frac{1}{E}T \quad (8)$$

If the system is carrying inertia J_2 only, then $E = Js^2$ and equation 8 results in:

$$\theta_2 = -\frac{1}{Js^2}T \quad (9)$$

Equation (9) resembles the Newton's law for the inertia J , under the torque of T . This means that for large values of H , the system will become totally backdrivable and responds to external torques, T , as if there was no harmonic drive in the system. (The system will not respond to R either since P will be very small for large values of H . One must choose a H such that the system responds both to R and T arbitrarily.) One cannot choose an arbitrarily large value for H ; the closed-loop stability of the system shown in Fig. 6 must be guaranteed.

5 Stability and Performance

The selection of H to shape the sensitivity function is not discussed here. Regardless of the type of the design method, it is important to notice the limitations that have evolved from the block diagram of Fig. 6:

1) If the system carries a mass only, then $E = Js^2$. The term Js^2 in the loop gain of Fig. 6 implies two zeros at the origin. (If G has an integrator, the pole/zero cancellation at the origin results in one zero for the loop gain.) The zeros at the origin do not let one choose a large value for H . This is true because term Js^2 results in a nonminimum phase loop transfer function with zeros at the center. Some control techniques may result in large values for H which drive the closed-loop poles to the open loop zeros located at the origin of the complex plane. In other words, a totally backdrivable system by choosing a large H (as described by Eq. (8)) cannot be achieved.

2) Another concern about the system arises when this harmonic drive is used to control the torque, W , in a torque control system [7]. Inspection of block diagram of Fig. 6 results in the following equation for the measured torque, W :

$$W = \frac{EG}{r + EGH}R \quad (10)$$

It can be observed that at DC (steady state), since $E = 0$, W will be zero in response to a constant input, R . Therefore, regardless of the torque measuring technique, the steady-state measurement of the torque sensor in response to con-

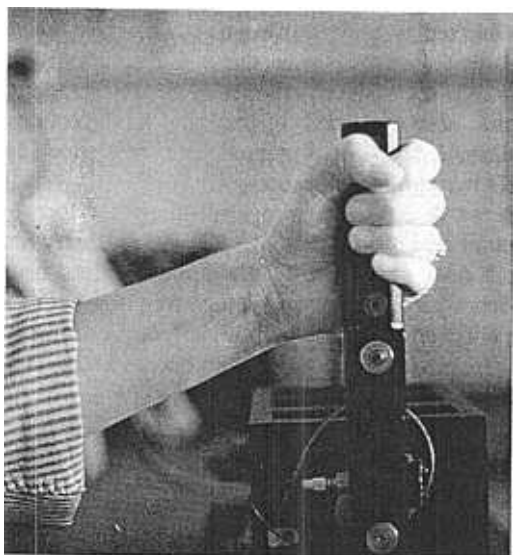


Fig. 7 Hand controller

stant inputs will be zero. This indicates that closed-loop torque control cannot be accomplished at DC. One might think of using an integrator for the controller H , to cancel the zero in the E . An integrator in the controller indicates an infinite value for input at DC. In practice this cannot be done since the actuator will saturate and the loop gain is still zero.

Note that the reason we are interested in the case of $E = J_2 s^2$ is due to the fact that we believe the system of motor-harmonic drive must remain stable in its simplest form of functioning: carrying a mass with inertia of J_2 . This inertia is at least equal to the inertia of the Rigid Circular Spline. The more elaborate case is when the link connected to Rigid Circular Spline interacts with an environment.

6 Experiments

A set of experiments was carried out on an active one-degree-of-freedom hand controller (Fig. 7).³ Hand controllers are powered joysticks that can be used by pilots. Hand controllers can also be used as master robots in telerobotic systems when rate-control governs the dynamics of the master robot. Another application for hand controllers can be found in maneuvering unmanned underwater vehicles where the operator maneuvers the vehicle from a mother ship using a hand controller. Traditionally, the speed of the underwater vehicle in various directions is a function of the position of the hand controller in various directions. The hand controller's range of motion usually is small: on the order of two-inch translational motion and $\pm 10^\circ$ rotational motion.

A closed-loop positioning controller was designed for the motor such that the widest bandwidth is achieved for G while the motor remains robust in the presence of its unmodeled dynamics. G is given by Eq. (12) resulting in approximate bandwidth of 2 rad/s.

$$G = \frac{125892.5}{s(s^2 + 140s + 4900) + 125892.5} \frac{\text{rad}}{\text{rad}} \quad (12)$$

³The hardware for construction of this hand controller was donated by CIMCORP located in Shoreview, Minnesota. The author appreciates this generosity.

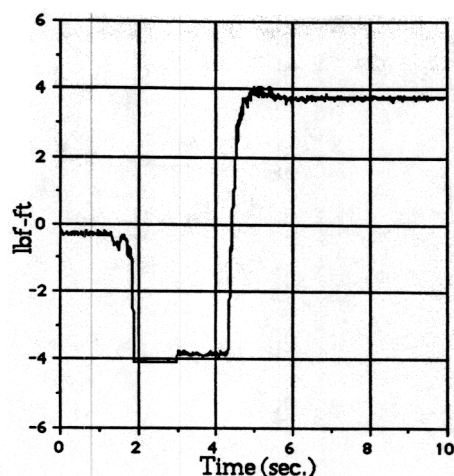


Fig. 8 The torque imposed by the pilot on the hand controller

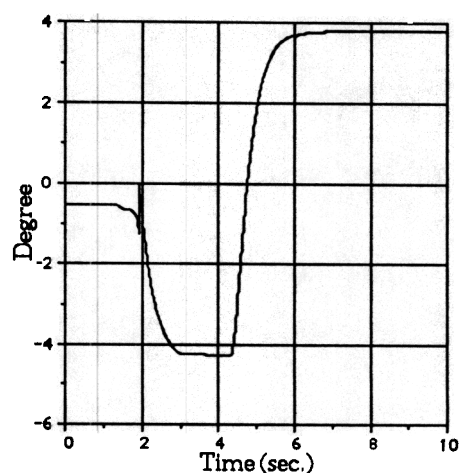


Fig. 9 The position of the hand controller

The inertia seen by the Rigid Circular Spline is $J_2 = 1.1534$ slug.ft² and $r = 201$. It is desired that the system exhibits a sensitivity of 1 degree/lbf-ft (or 0.01745 rad/lbf-ft) for widest possible bandwidth. In other words for every one lbf-ft exerted by a pilot, the stick should move 1 degree. This resembles the dynamic behavior of a spring. A set of experiments were carried out to demonstrate that the ratio of the stick motion, θ_2 , over the imposed torque, T , is in fact 1 degree/lbf-ft. Figure 8 shows the torque that the pilot imposed on the stick. The pilot first pulls about 4 lbf-ft and then pushes about 4 lbf-ft. Figure 9 represents the stick motion. Inspection of Figs. 8 and 9 shows that steady state torque of ± 4 lbf-ft results in ± 4 degree motion in the stick.

In another set of experiments, the pilot maneuvers the stick with a higher frequencies; Fig. 10 shows the torque imposed by the pilot on the stick. Fig. 11 shows the stick motion. It can be observed that the ratio of the stick position over the pilot torque for the first five seconds of the experiment is about 1 degree/lbf-ft while this ratio has been attenuated for the second five seconds of the experiment. This experiment shows that the target dynamics has been achieved only within the bandwidth of G only.

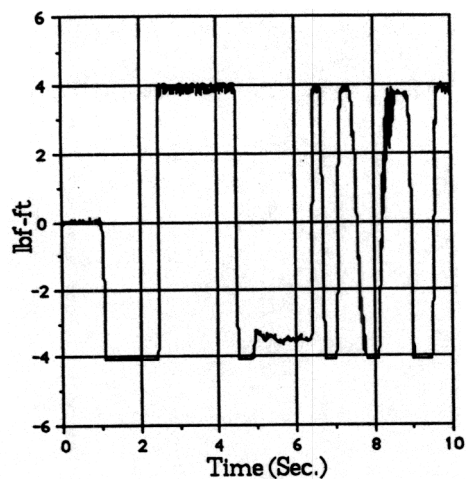


Fig. 10 The torque imposed by the pilot on the hand controller

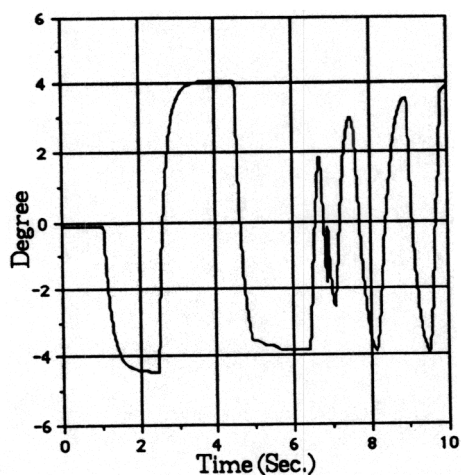


Fig. 11 The position of the hand controller is proportional with the imposed torque only at low frequencies

7 Conclusion

This article describes how a harmonic drive can be instrumented with force sensor to develop backdrivability. We have framed the harmonic drive backdrivability via a sensitivity transfer function. The sensitivity transfer function is defined as the transfer function that maps the external torques to the harmonic drive output position. It is shown that one cannot shape arbitrarily the system sensitivity function of a DC motor-harmonic drive. The more backdrivability is required, the smaller the stability range will be. It is also shown that closed loop torque control system cannot be achieved at DC.

References

- 1 Balas, G. J., Doyle, J. C., Glover, K., Packard, A., and Smith, R., " μ -Analysis and Synthesis Toolbox," The Math Works Inc, 1997.
- 2 de Silva, C. W., *Control, Sensors, and Actuators*, Prentice-Hall, Englewood Cliffs, NJ, 1989.
- 3 Hashimoto, M., Kiyosawa, Y., Paul, R. P., and Hirabayashi, H., "A Joint Torque Sensing for Robots with Harmonic Drives," *IEEE International Conference on Robotics and Automation*, Sacramento, CA, Apr. 1991.
- 4 Kazerooni, H., Waibel, B. J., and Kim, S., "Theory and Experiments on Robot Compliant Motion Control," *ASME JOURNAL OF DYNAMIC SYSTEMS, MEASUREMENT, AND CONTROL*, Sept. 1990.
- 5 Kazerooni, H., Guo, J., "Human Extenders," *ASME JOURNAL OF DYNAMIC SYSTEMS, MEASUREMENT, AND CONTROL*, Vol. 115, June 1993, pp 281-290.
- 6 Kazerooni, H., Tsay, and T.-I., Hollerbach, K., "A Controller Design Framework for Telerobotic Systems," *IEEE Control Systems Technology*, Vol. 1, No. 1, Mar. 1993, pp 50-62.
- 7 Pfeiffer, L., Khatib, O., and Hake, J., "Joint Torque Sensory Feedback in the Control of a PUMA Manipulator," *Proceedings of American Control Conference*, Seattle, WA, June 1986.
- 8 Woolvet, G. A., *Transducers in Digital Control of Dynamic Systems*, Addison-Wesley, Reading, MA, 1980.